Optimization of Silicon Solar Cell Efficiency Using SnO_2 and ZnO Anti-Reflective Coatings: A Numerical Approach with PC1D

Z. Amara[1,2], A. Benkhedda[1], M. Bouazza[1], R. Berkouk[1], A. Daikh[2,3*]

Abstract

A numerical simulation of the behavior of three types of solar cells: Si (N^+)/Si (P), SnO_2/Si (N^+)/Si (P), and ZnO/Si (N^+)/Si (P) is presented in this study. The simulation is devoted to analyzing the impact of the SnO_2 and ZnO window layers on the device's performance. We utilize a renowned photovoltaic modelling code, namely PC1D. A comparative analysis was conducted on the performance of the three structures Si (N^+)/Si (P), SnO_2 /Si (N^+)/Si (P), and ZnO /Si (N^+)/Si (P), assessing their impact on the characteristic I (V)/P(V) and efficiency, confirming an increase in conversion efficiency with the addition of the two anti-reflective layers, SnO_2 and ZnO, with efficiencies of 31.41% and 33.64% respectively.

1. University Centre of Naama, 45000, Algeria.
2. Artificial Intelligence Laboratory for Mechanical and Civil Structures, and Soil, University Centre of Naama, P.O. Box 66, Naama, 45000, Algeria
3. Laboratoire d'Etude des Structures et de Mécanique des Matériaux, Département de Génie Civil, Faculté des Sciences et de la Technologie, Université Mustapha Stambouli B.P. 305, R.P. 29000 Mascara, Algérie.
* Corresponding author: aadaikh@cuniv-naama.dz

1. Introduction

Semiconductors have been extensively studied due to their broad applications in science and technology (Kumar and Kahn, 2012). Silicon (Si) is a fundamental component in numerous electronic devices, especially in solar cells and integrated circuits. The foundation of the display industry relies on thin-film silicon photovoltaic technology (Shah et al.,1999). The reciprocal of the absorption coefficient of solar radiation must be less than the thickness of silicon due to its indirect band gap (Redfield, 1974; Escher and Redfield, 1974).

The effects of film growth temperature and post-deposition thermal annealing temperature on the optical and electrical properties of thin-film silicon solar cells were investigated (Park et al., 2015; El-Amin and Zaki, 2017). Si-doped indium tin oxides were investigated for their electrical and optical characteristics as clear Si-based solar cells' electrodes with anti-reflection coatings (Oh et al., 2015). Currently, average module efficiencies are around 17.5%, while commercial products have an efficiency record of 22.2% (Müller et al., 2017; Huang et al., 2017). Kaneka recently beat the efficiency record for research cells in 2017 with a verified result of 26.6% (Pandey and Chaujar, 2018; Ghannam and Abdulraheem, 2017). Because Auger recombination and intrinsic losses are taken into consideration, the theoretical limit for c-Si solar cells is 29.4%, meaning that only very minor performance enhancements are still possible (Egelhoff, 1987; Haschke et al., 2018; Bivour et al., 2014). The basic boundary of a single-junction solar cell is fundamentally constrained by the Shockley–Queisser limit. Passivating contacts enable the fabrication of high-performance Si solar cells by reducing recombination losses. Furthermore, upgrading Si with a high-bandgap tandem partner is a promising strategy to maximize solar spectrum utilization and achieve conversion efficiencies above 30%. This approach has the potential to surpass the efficiency of conventional single-junction solar cells (Zhou et al., 2022).

Environmental issues have grown more complex, and the world is facing significant energy-related challenges. Due to their environmental friendliness and long-term sustainability, solar cells are vital to the worldwide energy sector (Cai et al., 2018). Transparent conductive oxides (TCO), in particular, are known for their great transparency in the visible spectrum, large bandgap, and DC resistivity of up to 10^{-5}–10^{-4} Ω cm (n-type). Thin-film photovoltaic cells frequently employ them as front electrodes (Coleman and Jagadish, 2006). Different doping systems for binary and ternary oxides, include ZnO, CdO, SnO_2, In_2O_3, Cu_2O, Ga_2O_3, and $SrTiO_3$.

In order to enhance their optical and electrical properties, the materials SnO_2 and ZnO have been combined with supplementary semiconductors (Hussain et al., 2015; Labed et al., 2021; Aydın and Sığırcık, 2019).

Zinc oxide has emerged as a promising option for the implementation of transparent conductive oxides (TCO) in the photovoltaic (PV) industry. This is primarily attributed to its advantageous characteristics, including its low toxicity, cost-effectiveness, ability to be deposited at low temperatures, abundance in nature, and potential for reducing production expenses (Tohoda et al., 2012; Korte et al., 2009). It is classified as an n-type semiconductor with a band gap energy of 3.2 electron volts (eV). It possesses a notable exciton binding energy of 60 millielectron volts (meV) (Alfaro Cruz et al., 2018; Oleshkevych et al., 2014; Garza-Hernández et al., 2020; He et al., 2015; Rahman et al., 2022).

Several researchers have used n-ZnO thin films since the material was adopted as an emitter layer in an effort to produce solar cells that may be both inexpensive and highly efficient. The proposal of an antireflection (AR) coating has been put out (Hussain et al., 2015; Sikder and Asif, 2016). Due to the significant importance of the optical properties of ZnO in its role as a front n-layer, it is anticipated that the front ZnO film will serve as both an anti-reflection coating and an electrically active layer in the fabrication of p-n junctions. Hetero p-n junction solar cells have several advantages, including the ability to select materials, adjust layer thickness, control dopant concentrations, implement intrinsic surface passivation, and employ low-temperature techniques (Hussain et al, 2015). Therefore, it is plausible that zinc oxide silicon heterojunction solar cells might exhibit enhanced competitiveness within the photovoltaic sector in the next years. Several groups have also successfully developed metal oxide-based solar cells using single Si heterojunctions (Tyagi et al., 2022).

Transparent conductive oxides (TCOs) are a group of materials that includes tin dioxide (SnO_2). The use of this material as a transparent electrical contact in many fields, such as electronics, optics, and catalysis, is highly advantageous owing to its non-toxic nature and the abundant availability of its constituent elements on our planet. Tin dioxide (SnO_2) is classified as an n-type semiconductor due to its electronic properties, characterized by a band gap above 3.0 eV. The stability of SnO2 thin films is contingent upon the existence of defects and impurities inside the material, as shown by several sources (Li et al., 2020, Rani et al., 2020, Bousmaha et al., 2019, Zhao et al., 2019).

A solar cell's anti-reflective coating (ARC) layer preserves the cell from environmental deterioration while assisting in light absorption (Sarkin et al., 2020, Tiwari et al., 2021). In the absence of the anti-reflective coating (ARC) layer, the cells exhibit a natural dark grey color. Nevertheless, the color of the solar cells may be altered by manipulating the thickness of the ARC layer (Hu et al., 2021, Shah et al., 2020). One of the primary challenges in attaining optimal efficiency lies in the optical losses that occur at the front surface of the solar cell (Battaglia et al., 2016). In order to mitigate optical losses resulting from reflection and optimize light transmission, a thin layer of dielectric material, commonly referred to as an anti-reflective coating (ARC), is applied to the illuminated surface of the solar cell. This results in an improvement in the existing production process and the overall operational effectiveness of the solar cell.

To investigate the improvement in power conversion efficiency, we employed ZnO and SnO_2 as an antireflection coating on a silicon solar cell. The thickness of ZnO and SnO_2 layers has been tuned to increase solar cell performance with various substrates.

In this paper, we will report simulation-based optimization of three solar cells using PC1D software, which are cell homojunction Si (N+)/Si (P) and two cells heterojunction SnO_2 /Si (N+)/Si (P), ZnO/Si (N+)/Si (P), where SnO_2 and ZnO used as an anti-reflective layer. The Si (N+)/Si(P) homojunction cell's parameters will be optimized in the first section of this study. We'll figure out the best values for the following parameters: the area surface, the thickness of the n-region, the application of texturization to the front surface to cut down on reflection losses, and the angle and depth of the texturization. To emphasize the value of ARLs (Anti-Reflection Layers) on silicon solar cells, SnO_2 and ZnO will be included as antireflection layers in the second section.

2. Device structure and modeling parameters

2.1. Device structure

This section introduces the concepts of personal computer one-dimensionality (PC1D), which serve as the basis for simulation calculations. PC1D is a finite-element software application utilized for the simulation of semiconductor devices, employing finite elements as its computational framework.

The first simulated structure solar cell, N-Si/P-Si, is depicted in Figure 1.

The efficiency refers to the percentage of the incident solar energy that the module is able to convert into usable electrical energy, and it's also the ratio of the power generated by the cell.

$$P = V\ x\ I \tag{1}$$

The form factor FF indicates how the shape of the I(V) curve affects the performance of the cell. A closer match to a rectangular shape results in a higher FF, which is closer to 1.

$$FF = \frac{P_{max}}{P_1} = \frac{V_m \times I_m}{V_{co} \times I_{cc}} \tag{2}$$

This leads to :

$$\eta = \frac{P_{max}}{P_0} \tag{3}$$

With:

I_{cc} : Short-circuit current.

V_{co} : Short-circuit voltage.

P_{max} : Max base power out.

P_1 : Power of the incident solar radiation.

FF : Form Factor.

η : Efficiency

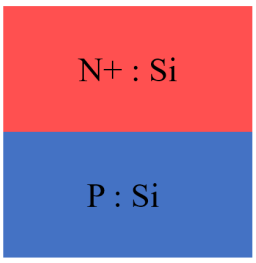

Fig.1. Schematic of Si solar cell.

The second simulated solar cell is SnO2/Si(N+)/Si(P), which is presented in Figure 2. Adding a layer of SnO2 to the Si solar cell can potentially improve its efficiency by reducing the amount of light that is reflected and increasing the amount of light that is absorbed. The numerical values of the parameters for the SnO2/Si(N+)/Si(P) heterojunction are provided in Table 1.

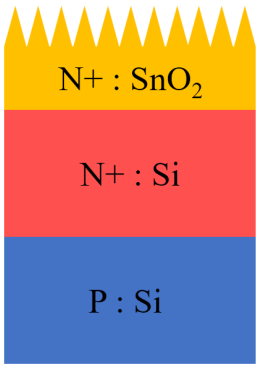

Fig.2. Schematic of the SnO2/Si(N+)/Si(P) heterojunction solar cell.

The third simulated solar cell is ZnO/Si(N+)/Si(P) (see Figure 3). ZnO is considered an antireflective layer for Si Solar cells. The input parameters are presented in Table 2.

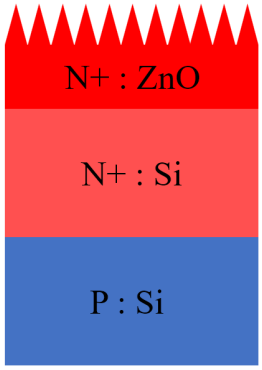

Fig.3. Schematic of the ZnO/Si(N+)/Si(P) heterojunction solar cell.

2.2. Modeling parameters

The simulated structure's solar cell is constructed using PC1D Ver. 6.2. We have changed the cross-sectional area to three values [100 cm^2; 120 cm^2; 150 cm^2; 200 cm^2] of the first structure, N-Si/P-Si. It is conducted with a singular solar intensity of 0.1 W/cm^2 and an air mass of AM1.5. The excitation of the carrier is partitioned into 16 discrete time intervals, while the surrounding temperature is established at 25°C. Parameters of the concentration are N-type background doping: 10^{17} cm^{-3} and P-type background doping:10^{15} cm^{-3}.

Tables below represent the modeling parameters of our simulated solar cells with antireflective layers SnO_2 and ZnO, respectively, by fixing the device area of 16 cm^2:

Table 1. Parameters of the SnO_2/Si(N+)/Si(P) heterojunction solar cell.[48]

Device area	16cm²
Front surface texture angle	110°
Front surface texture depth	4μm
1st device region	Layer SnO2
Electron mobility	25cm²/Vs
Hole mobility	2500cm²/Vs
Dielectric constant	9
Gap Energy	3.8 eV
Intrinsic concentration at 300K	10^{-14} cm^{-3}
Refractive index	1.9
F-type background doping	1×10^{17} cm^{-3}
Bulk recombination	$\boldsymbol{\tau n = \tau p = 1000}$μs
2nd device region	Junction Si(N^+)
Thickness	30μm
Electron mobility	from internal model of silicon
Dielectric constant	11.9
Gap energy	1.124eV
Intrinsic concentration at 300K	10^{10} cm^{-3}
Refractive index	3.58
Absorption coefficient	si300.abs
N-type background doping	1×10^{17} cm^{-3}
Bulk recombination	$\boldsymbol{\tau n = \tau p = 3000}$μs
3rd device region	Junction Si(P)
Thickness	10μm
P-type background doping	1×10^{15} cm^{-3}
Bulk recombination	$\boldsymbol{\tau n = \tau p = 3000}$μs
Excitation	from one-sun.exc

Table 2. Parameters of the ZnO/Si(N+)/Si(P) heterojunction solar cell. [50]

Device area	16cm²
Front surface texture angle	110°
Front surface texture depth	4µm
1st device region	Layer ZnO
Dielectric constant	8.66
Gap Energy	3.27eV
Intrinsic concentration at 300K	10^{-14} cm^{-3}
Refractive index	2
F-type background doping	1×10^{17} cm^{-3}
2nd device region	Junction Si(N^{+})
Thickness	30µm
Dielectric constant	11.9
N-type background doping	1×10^{17} cm^{-3}
3rd device region	Junction Si(P)
Thickness	10µm
P-type background doping	1×10^{15} cm^{-3}

3. Results and discussions

3.1 Influence of the area surface on the characteristic I-V/Power:

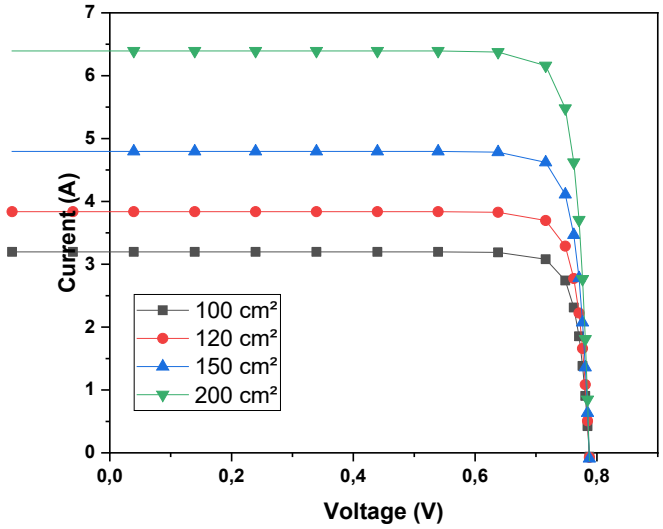

Fig.4. Influence of the area surface on the I-V characteristic.

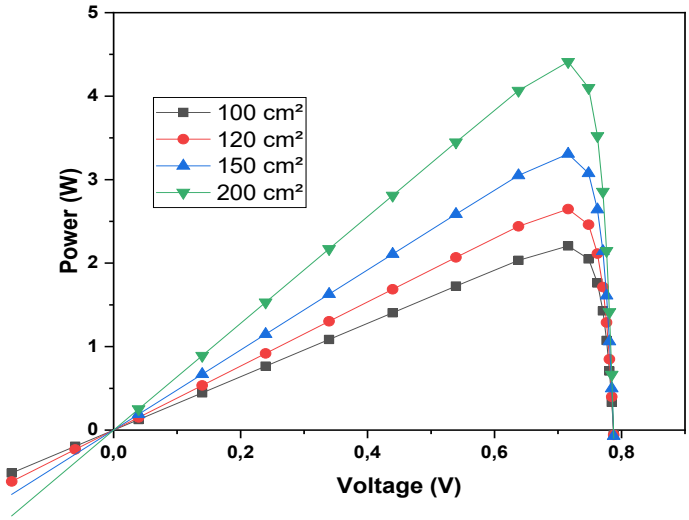

Fig.5. Influence of the area surface on the P-V characteristics.

Figures 4 and 5 illustrate the impact of surface area on the I (V) and P (V) curves, respectively. The P (V) curve illustrates a pattern where the power output rises to a maximum and thereafter declines. The apex of the power curve signifies the utmost level of power that the cell is capable of generating. We initiated an inquiry into the potential influence of the surface area of the solar cell on power generation. By altering the surface area of a solar cell, we are essentially modifying the quantity of sunlight that the cell is able to gather. Expanding the surface area of the solar cell enables it to capture a greater amount of sunlight, resulting in higher power production as indicated in Table 3. With an increase in surface area, there will be a corresponding rise in output power. (Belarbi et al., 2014) The information provided is insufficient. Our examination of the I-V characteristics indicates that the increase in power is mostly due to an elevation in the current magnitude (which is controlled by the photo-current and, consequently, the amount of light received) as the surface area expands. This is due to the fact that the voltage remains relatively constant despite variations in surface area. Increasing the size of the cell area can result in the addition of more electron channels and transporters on the cell surface. This can lead to a decrease in the electrical resistance of the cell membrane and an increase in the electrical current flowing through it (as shown in the table). In addition, the augmented surface area can lead to a larger effective area for electron transfer, hence enhancing their flow. The efficiency of a solar cell is determined by the correlation between the amount of sunlight it receives and its output of electrical power. The outcome is contingent upon various elements, including the bandgap energy of the semiconductor material, the efficacy of the separation and collection of electron-hole pairs, and the reflectivity of the cell surface. By enlarging the surface area of a solar cell, we enhance its capacity to capture a greater quantity of sunlight. The increase in sunlight results in an increase in the number of electron-hole pairs that can be produced, leading to a higher electrical power output.

Table 3. Optimized parameters of the homojunction Si(N)/Si(P) solar cell.

Device area	100	120	150	200
Icc (A)	-3.197	-3.837	-4.796	-6.395
Vco (V)	0.7874	0.7874	0.7874	0.7874
Pmax (W)	2.206	2.647	3.308	4.411
FF	0.8763	0.8761	0.8759	0.8759
***η* (%)**	22.06	22.06	22.06	22.06

SnO_2/Si(N+)/Si(P) solar cell:

Table 4 summarizes the efficiency results obtained for the different thicknesses of the anti-reflective layer (ARL) with SnO_2, ranging from 0.10µm to 0.30µm. The corresponding efficiency values were found to be 28.80%, 29.61%, 30.76%, and 31.41% respectively. As shown in Table 4, the efficiency of the solar cell increased with increasing thickness of the anti-reflective layer SnO_2. Furthermore, the current and the power increased, this can be more clearly visualized in the Figures (6) and (7) respectively.

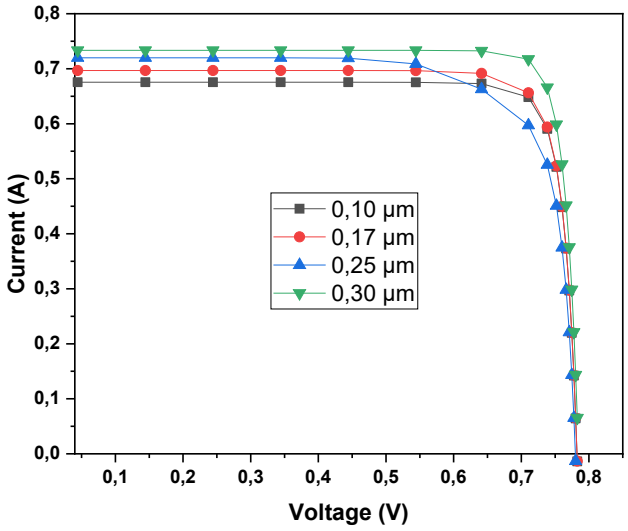

Fig.6. Influence of the thickness of SnO_2 region on the I-V characteristics. (*a*) 0.10*µm*, (*b*) 0.17*µm*, (*c*) 0.25*µm*, (*d*) 0.30*µm*.

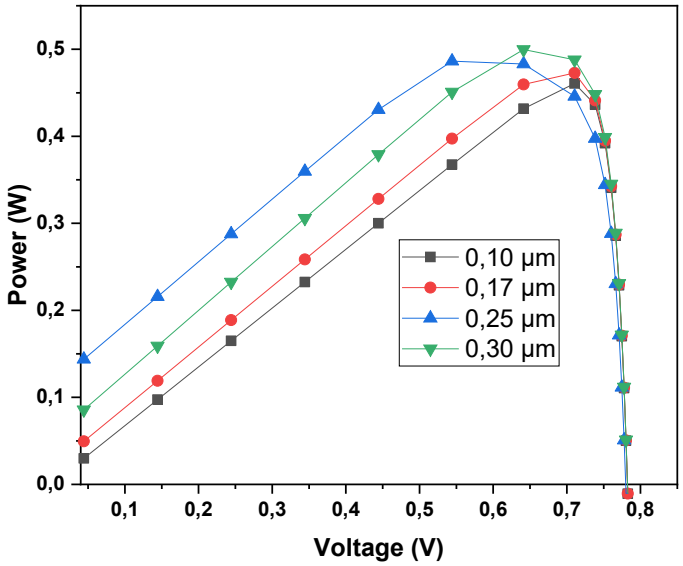

Fig.7. Influence of the thickness of SnO_2 region on the P-V characteristics.

(*a*) 0.10*µm*, (*b*) 0.17*µm*, (*c*) 0.25*µm*, (*d*) 0.30*µm*.

Table 4. Comparison of the different thicknesses of ARL in the SnO_2 region.

Thickness of	**0.10**	**0.17**	**0.25**	**0.30**
Icc (A)	-0.675	-0.696	-0.720	-0.733
Vco (V)	0.7823	0.7828	0.7833	0.7836
Pmax (W)	0.4608	0.4738	0.4921	0.5026
FF	0.8726	0.8696	0.8725	0.8750
***η* (%)**	28.80	29.61	30.76	31.41

The highest value of efficiency was obtained with a 0.30µm thickness of the antireflective layer. This value was greater than the result obtained by R. Tala-Ighil et al (Tala-Ighil and Boumaour, 2007). The solar cell with a SnO2 antireflecting coating sheet 0.30µm thick achieved a maximum conversion efficiency (η) of 31.41 %. The table demonstrates that, in general, the anti-reflective properties of a thicker SnO2 layer can be better, leading to a higher current and efficiency in the solar cell and more light transmission. This was also observed by Habubi et al. who studied an experimental result (Habubi et al., 2019).

ZnO/Si(N+)/Si(P) solar cell:

Using the aforementioned parameters for the simulation, we varied the thickness as follows: 1µm; 2µm; 3µm; 4µm. The following results were obtained from the simulated cell.

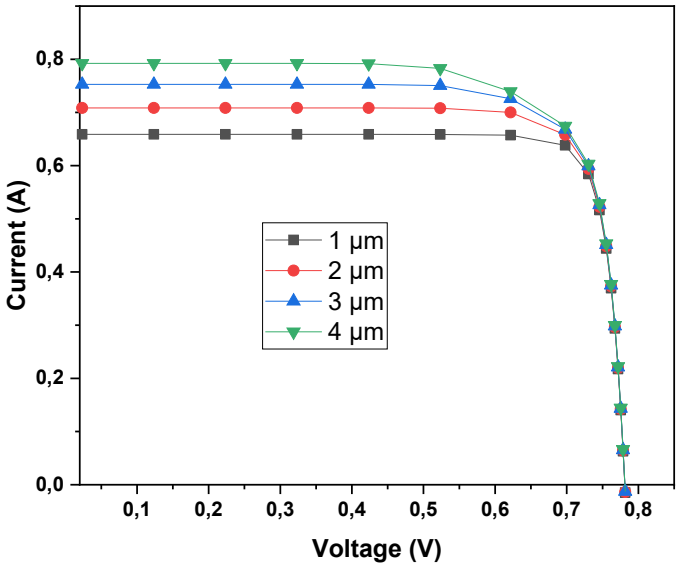

Fig. 8. Influence of the thickness of ZnO region on the I-V characteristics.

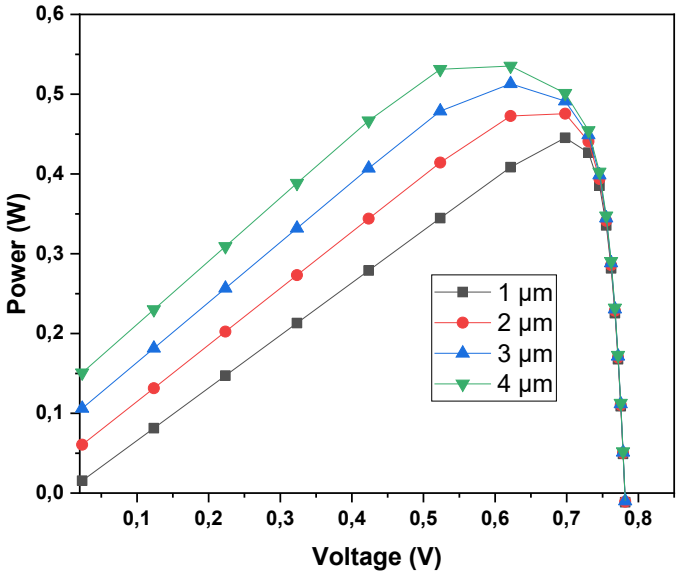

Fig. 9. Influence of the thickness of ZnO region on the P-V characteristics.

Table 5. Comparison of the different thicknesses of ARL in the ZnO region.

Thickness of	1	2	3	4
Icc (A)	-0.6587	-0.7084	-0.7527	-0.7922
Vco (V)	0.7811	0.7823	0.7836	0.7848
Pmax (W)	0.4461	0.4789	0.5135	0.5382
FF	0.8670	0.8641	0.8706	0.8656
***η* (%)**	27.88	29.93	32.09	33.64

The results obtained from our study on the effect of varying the thickness of a ZnO anti-reflective layer (ARL) on the efficiency of a solar cell are summarized in Table 5 and illustrated in Figures 8 and 9. As shown, increasing the thickness of the ZnO ARL from 1μm to 4μm led to a steady increase in efficiency from 27.93% to 33.66% respectively. These results demonstrate the potential of the ZnO ARL as an effective means of increasing the efficiency of solar cells.

The increase in efficiency observed in our study can be attributed to the ability of the ZnO ARL to reduce the amount of light that is reflected at the surface of the solar cell. As the thickness of the ZnO ARL increases, more light is absorbed by the layer, leading to a greater amount of power generated. Our results are consistent with previous studies that have demonstrated the effectiveness of ZnO ARLs in improving solar cell efficiency (Naim et al., 2022; Taguchi et al., 2014; Mishima et al., 2011; Tsunomura et al., 2009). However, the optimal thickness of the ZnO ARL reported in our study (4μm) is much more promising than that reported in the study mentioned.

The thicknesses used in our simulations align well with experimentally deposited layers via spray pyrolysis or hydrothermal methods, suggesting practical feasibility. Comparing the efficiency results to theirs, they found an efficiency of 24.8% which is inferior to ours. This is because we investigated the influence of multiple parameters and we took the perfect one from each parameter in order to seek a higher efficiency value.

The superior antireflective performance of ZnO can be explained by its refractive index (~2 at 600 nm), which closely matches the optimal value calculated as the geometric mean between air (n=1) and silicon (n≈4). This index matching reduces reflection at the interface. Furthermore, the optimal ZnO ARL thickness (~76–80 nm) aligns with our simulated best-performing values, reinforcing the physical basis of our efficiency gain, and is observed in the study of Askari and Das, 2017. This clearly demonstrates that ZnO offers a physical optical advantage thanks to a well-matched refractive index. These results establish consistency between the wavelength (600 nm), the optimal index (~2), and the ideal layer thickness (~76 nm).

The high efficiency obtained in simulations, particularly with ZnO ARLs, is consistent with other experimental studies of ZnO nano-whisker coated Si solar cells (Yu et al., 2012) demonstrating a relative efficiency improvement of approximately 29% under AM1.5 illumination. Furthermore, other work (Lai et al., 2020) studied the improvement of amorphous silicon thin-film photovoltaic cells with Zinc Oxide Nanorods, and they obtained an efficiency enhanced to 29 %. However, it is essential to note that real-world devices are subject to additional parasitic losses (e.g., surface recombination, contact resistance) that may reduce their effective performance.

Conclusion

The focus of our research is to simulate three types of solar cells using PC1D software. These include a homojunction Si (N^+)/Si (P) cell, as well as two heterojunction cells with anti-reflective layers made of SnO_2/Si (N^+)/Si (P) and ZnO/Si (N^+)/Si (P). In the first phase, we incorporated SnO_2 and ZnO as anti-reflective layers (ARLs) to emphasize the significance of ARLs in silicon solar cells. We examined the impact of ARL thickness on the textured solar cell and utilized experimental data on absorption coefficient and refractive index of SnO_2 and ZnO. The modelling findings demonstrate that the incorporation of SnO2 and ZnO on the surface of the homojunction solar cell significantly enhances the conversion efficiency. The percentage increases from 26% to 31% for SnO2 and from 26% to 33% for ZnO.

References

Alfaro Cruz, M.R., Garza-Hernández, R., Horley, P.P., Mata-Ramírez, E., Martínez-Guerra, E. and Aguirre-Tostado, F.S. (2018). Low temperature ZnO films grown by successive ionic layer adsorption and reaction method. *Thin Solid Films.*

Ali, A.M., Ismail, A.A., Najmy, R. and Al-Hajry, A. (2014) Preparation and characterization of ZnO-SiO_2 thin films as highly efficient photocatalyst. *Journal of Photochemistry and Photobiology A: Chemistry.*

Askari, S.S.A. & Das, M.K. (2017) *Computer, Communication and Electrical Technology* – Guha, Chakraborty & Dutta (Eds)Taylor & Francis Group, ISBN 978-1-138-03157-9.

Aydın, E.B. and Sığırcık, G. (2019) Preparations of different ZnO nanostructures on TiO_2 nanotube via electrochemical method and its application in hydrogen production. *International Journal of Hydrogen Energy.*

Battaglia, C., Cuevas, A., and De Wolf, S. (2016) High-efficiency crystalline silicon solar cells: Status and perspectives. *Energy and Environmental Science*, 9, 1552–1576.

Belarbi, M., Benyoucef, A., Benyoucef. B. (2014) Simulation of the solar cells with PC1D, application to cells based on Silicon. *Advanced Energy: An International Journal (AEIJ)*, Vol. 1, No. 3.

Bivour, M., Schröer, Hermle, M. and Glunz, S.W. (2014). Silicon heterojunction rear emitter solar cells: less restrictions on the optoelectrical properties of front side TCOs. *Solar Energy Materials and Solar Cells.*

Bousmaha, M., Bezzerrouk, M.A., Kharroubi, B., Akriche, A., Naceur, R., Hattabi, I. and Sandjak-Eddine, K. (2019) Enhanced photocatalysis by depositing ZnO thin film in the inner wall of glass tube. *Optik.*

Cai., X., Zhou, X., Liu, Z., Jiang, F. and Yu, Q. (2018). An in-depth analysis of the silicon solar cell key parameters' optimal magnitudes using PC1D simulations. *Optik* (2018)

Coleman, V.A. and Jagadish, C. (2006). Basic properties and applications of ZnO. *Thin Films and Nanostructures.*

Egelhoff, W.F., Jr. (1987). Core-level binding-energy shifts at surfaces and in solids. *Surface Science Reports.*

El-Amin, A.A. and Zaki, A.A., (2017). Improving the Efficiency of multicrystalline silicon by adding an ARC layer in the front device, *Silicon* 9, 53–58.

Escher, J.S. and Redfield, D., (1974). Analysis of carrier collection efficiencies of thin-film silicon solar cells. *Applied Physics Letters*, 25 (1974) 702.

Garza-Hernández, R., Lugo-Laredo, S. and Aguirre-Tostado, F.S., (2020) The role of copper during the growth of stoichiometric Cu_2ZnSnS_4 by successive ionic layer adsorption and reaction method. *Ceramics International.*

Ghannam, M. and Abdulraheem, Y. (2017). Fundamental constraints imposed by energy barriers on the fill factor and on the efficiency of silicon heterojunction solar cells. *Solar Energy Materials and Solar Cells.*

Habubi, N.F., Ismail, R.A., Mishjil, K.A. and Hassoon, K.I. (2019) Increasing the silicon solar cell efficiency with nanostructured anti-reflecting coating films, *Silicon* 11:543–548(2019). DOI.org/article/10.1007/s12633-017-9727-6.

Haschke, J., Dupré, O., Boccard, M. and Ballif, C. (2018). Silicon heterojunction solar cells: recent technological development and practical aspects - from lab to industry. *Solar Energy Materials and Solar Cells.*

He, Y., Wang, Y., Zhang, L., Teng, B. and Fan. M. (2015) High-efficiency conversion of CO_2 to fuel over ZnO/g-C_3N_4 photocatalyst. *Applied Catalysis B: Environmental.*

Hu, R., Li, Y., Que, Z., Zhai, S., Feng, Y., Chu, L. and Li, X. (2021) Low Temperature VOx Hole Transport Layer for Enhancing the Performance of Carbon-Based Perovskite Solar Cells. *Journal of Nanoelectronics and Optoelectronics*, 16, 273–280.

Huang, H., Lv, J., Bao. Y., Xuan, R., Sun, S., Sneck, S., Li, S., Modanese, C., Savin, H., Wang, A. and Zhao, J. (2017). 20.8% industrial PERC solar cell: ALD Al_2O_3 rear surface passivation, efficiency loss mechanisms analysis and roadmap to 24%. *Solar Energy Materials and Solar Cells*.

Hussain, B., Ebong, A., and Ferguson, I. (2015) *2015 IEEE 42nd Photovoltaic Specialist Conference (PVSC), 1–4.*

Hussain, B., Ebong, A. and Ferguson, I. (2015). Zinc oxide as an active n-layer and antireflection coating for silicon based heterojunction solar cell. *Solar Energy Materials and Solar Cells.*

Korte, L., Conrad, E., Angermann, H., Strangl, R. and Schmidt, M. (2009) Solar energy material & amp. *Solar Cells.*

Kumar, S. and Khan, M.A.M., (2012). *Chalcogenide Letters*, 9, 145–149.

Labed, M., Sengouga, N., Meftah, A., Meftah, A. and Rim, Y.S. (2021) Study on the improvement of the open-circuit voltage of NiOx/Si heterojunction solar cell. *Optical Materials.*

Lai, F-I, Yang, J-F, Hsu, Y-C, and Kuo, S-Y. (2020) Crystals, 10, 1124. doi:10.3390/cryst10121124

Li, Z., Yang, H., Zhang, L., Liu, R. and Zhou, Y. (2020) Stainless steel mesh-supported three-dimensional hierarchical SnO_2/Zn_2SnO_4 composite for the applications in solar cell, gas sensor, and photocatalysis. *Applied Surface Science*.

Mishima, T., Taguchi, M., Sakata, H., and Maruyama, E. (2011) *Solar Energy Materials and Solar Cells,* 95, 18 doi.org/10.1016/j.solmat.2010.04.030

Müller, M., Fischer, G., Bitnar, B., Steckemetz, S., Schiepe, R., Mühlbauer, M., Köhler, R. and Richter, P. (2017). Loss analysis of 22% efficient industrial PERC solar cells. *Energy Procedia*.

Naim, H., Shah, D.K., Bouadi, A., Siddiqui, M.R., Akhtar, M.S., Kim, C.Y. (2022). Journal of Electronic Materials. DOI.org/10.1007/s11664-021-09341-5.

Ogugua, S.N., Ntwaeaborwa, O.M. and Swart, H.C. (2021). Luminescence, structure and insight on the inversion degree from normal to inverse spinel in a $ZnAl_{(2-x)}Fe_x^{3+}O_4$ system. *Boletin de la Sociedad Española de Cerámica y Vidrio.*

Oh, G., Lee, K.S. and Kim, E.K., (2015). Electrical and optical properties of Si-doped indiumtin oxides as transparent electrode and anti-reflection coating for solar cells. *Current Applied Physics* 15, 794–798.

Oleshkevych, A.I., Voloshko, S.M. and Sidorenko, S.I. (2014) Enhanced diffusion caused by surface reactions in thin films of Sn-Cu-Mn. *Thin Solid Films.*

Pandey, R. and Chaujar, R. (2018). Rear contact silicon solar cells with a-SiC_X:H based front surface passivation for near-ultraviolet radiation stability. *Superlattices and Microstructures*.

Park, J., Shin, C., Lee, S., Kim, S., Jung, J., Balaji, N., Dao, V.A., Lee, Y.-J. and Yi, J. (2015) Effect of thermal annealing on the optical and electrical properties of boron doped a-SiOx: H for thin-film silicon solar cell applications. *Thin Solid Films* 587, 132–136.

Rahman, M., Kamruzzaman, M., Zapien, J. A., Afrose, R., Anam, T.K., Liton, N.M.H., Helal, M.A. and Khan, M.K.R. (2022) Conversion of n-type to p-type conductivity in ZnO by incorporation of Ag and Ag–Li. *Materials Today Communications, 33*, 104278.

Rani, A., Singh, K., Patel, A.S., Chakraborti, A., Kumar, S., Ghosh, K. and Sharma, P. (2020) Visible light driven photocatalysis of organic dyes using SnO_2 decorated MoS_2 nanocomposites. *Chemical Physics Letters.*

Redfield, D., (1974). Multiple-pass thin-film silicon solar cell. *Applied Physics Letters*, 25, 647.

Sarkın, A.S., Ekren, N. and Sa˘glam, Ş. (2020) A review of anti-reflection and self-cleaning coatings on photovoltaic panels. *Solar Energy*, 199, 63–73.

Sefardjella, H., Boudjema, B. and Kabir, A. (2013). Structural and photoluminescence properties of SnO_2 obtained by thermal oxidation of evaporated Sn thin films. *Current Applied Physics.*

Shah, A., Torres, P., Tscharner, R., Wyrsch,N. and Keppner, H., (1999). Photovoltaic technology: the case for thin-film solar cells. *Science 285*, 692–698.

Shah, D.K., Son, Y.-H., Lee, H.-R., Akhtar, M.S., Kim, C.Y., and Yang, O.-B. (2020) A stable gel electrolyte based on poly butyl acrylate (PBA)-co-poly acrylonitrile (PAN) for solid-state dye-sensitized solar cells. *Chemical Physics Letters*, 754, 137756.

Sikder, U. and Asif, M. (2016) *Optics and Laser Technology*. 79, 88.

Taguchi, M., Yano, A., Tohoda, S., Matsuyama, K., Nakamura, Y., Nishiwaki, T., Fujita, K., and Maruyama, E. (2014) IEEE Journal of Photovoltaics, 4, 96.
DOI: 10.1109/JPHOTOV.2013.2282737

Tala-Ighil, R. and Boumaour, M. (2007) Numerical simulation of silicon based solar cells with a degenerated SnO2:F window layer, *The European Physical Journal-Applied Physics*, 40, 253–256. DOI: 10.1051/epjap:2007158.

Tiwari, R., Sadanand, Dubey, P., Lohia, P., Dwivedi, D.K., Fouad, H. and Akhtar, M.S. (2021) Simulation Engineering in Quantum Dots for Efficient Photovoltaic Solar Cell Using Copper Iodide as Hole Transport Layer. *Journal of Nanoelectronics and Optoelectronics*,16, 1897–1904.

Tohoda, S., Fujishima, D., Yano, A., Ogane, A., Matsuyama, K., Nakamura, Y., Tokuoka, N., Kanno, H., Kinoshita, T., Sakata, H., Taguchi, M. and Maruyama, E. (2012) Future directions for higher-efficiency HIT solar cells using a Thin Silicon Wafer. *Journal of Non-Crystalline Solids.*

Tsunomura, Y., Yoshimine, Y., Taguchi, M., Baba, T., Kinoshita, T., Kanno, H., Sakata, H., Maruyama, E., and Tanaka, M. (2009) *Solar Energy Materials and Solar Cells*, 93, 670.

Tyagi, S., Singh, P.K. and Tiwari, A.K. (2022) Photovoltaic parameter extraction and optimisation of ZnO/GO based hybrid solar trigeneration system using SCAPS 1D. *Energy for Sustainable Development.*

Yu, X., Wang, D., Lei, D., Li, G., and Yang, D. (2012) *Nanoscale Research Letters*, 7:306. doi: 10.1186/1556-276X-7-306

Zhao, B., Mattelaer, F., Kint, J., Werbrouck, A., Henderick, L., Minjauw, M., Dendooven, J. and Detavernier, C. (2019) Atomic layer deposition of ZnO-SnO_2 composite thin film : the influence of structure, composition and crystallinity on lithium-ion battery performance. *Electrochimica Acta.*

Zhou, J., Huang, Q., Ding, Y., Hou, G., and Zhao, Y. (2022). Passivating contacts for high-efficiency silicon-based solar cells: From single-junction to tandem architecture. *Nano Energy*, 92, 106712.